OPEN ACCESS

Original research

A mucus production programme promotes classical pancreatic ductal adenocarcinoma

Claudia Tonelli,[1] Georgi N Yordanov,[1] Yuan Hao,[1] Astrid Deschênes,[1] Juliene Hinds,[1] Pascal Belleau,[1] Olaf Klingbeil,[1] Erin Brosnan,[1] Abhishek Doshi,[1] Youngkyu Park,[1] Ralph H Hruban,[2] Christopher R Vakoc,[1] Alexander Dobin,[1] Jonathan Preall,[1] David A Tuveson[1,3]

► Additional supplemental material is published online only. To view, please visit the journal online (http://dx.doi.org/10.1136/gutjnl-2023-329839).

[1]Cold Spring Harbor Laboratory, Cold Spring Harbor, New York, USA
[2]Department of Pathology, Johns Hopkins University School of Medicine, Baltimore, Maryland, USA
[3]Lustgarten Foundation Pancreatic Cancer Research Laboratory, Cold Spring Harbor, New York, USA

Correspondence to
Dr David A Tuveson, Cold Spring Harbor Laboratory, Cold Spring Harbor, NY 11724, USA; dtuveson@cshl.edu

Received 9 March 2023
Accepted 9 January 2024

To cite: Tonelli C, Yordanov GN, Hao Y, *et al*. *Gut* Epub ahead of print: [*please include* Day Month Year]. doi:10.1136/gutjnl-2023-329839

ABSTRACT

Objective The optimal therapeutic response in cancer patients is highly dependent upon the differentiation state of their tumours. Pancreatic ductal adenocarcinoma (PDA) is a lethal cancer that harbours distinct phenotypic subtypes with preferential sensitivities to standard therapies. This study aimed to investigate intratumour heterogeneity and plasticity of cancer cell states in PDA in order to reveal cell state-specific regulators.

Design We analysed single-cell expression profiling of mouse PDAs, revealing intratumour heterogeneity and cell plasticity and identified pathways activated in the different cell states. We performed comparative analysis of murine and human expression states and confirmed their phenotypic diversity in specimens by immunolabeling. We assessed the function of phenotypic regulators using mouse models of PDA, organoids, cell lines and orthotopically grafted tumour models.

Results Our expression analysis and immunolabeling analysis show that a mucus production programme regulated by the transcription factor SPDEF is highly active in precancerous lesions and the classical subtype of PDA — the most common differentiation state. SPDEF maintains the classical differentiation and supports PDA transformation *in vivo*. The SPDEF tumour-promoting function is mediated by its target genes AGR2 and *ERN2*/IRE1β that regulate mucus production, and inactivation of the SPDEF programme impairs tumour growth and facilitates subtype interconversion from classical towards basal-like differentiation.

Conclusions Our findings expand our understanding of the transcriptional programmes active in precancerous lesions and PDAs of classical differentiation, determine the regulators of mucus production as specific vulnerabilities in these cell states and reveal phenotype switching as a response mechanism to inactivation of differentiation states determinants.

WHAT IS ALREADY KNOWN ON THIS TOPIC

⇒ Pancreatic ductal adenocarcinoma (PDA) cells exist as dynamic cell states underlying intratumour heterogeneity.
⇒ Classical PDA cells are characterised by high mucin production.
⇒ In secretory cells, the transcription factor SPDEF regulates several proteins involved in mucus production, including AGR2 and *ERN2*/IREβ.

WHAT THIS STUDY ADDS

⇒ Precancerous lesions and PDAs of the classical subtype activate a mucus production programme regulated by SPDEF.
⇒ Impairment of the SPDEF programme reduces the growth of classical subtype PDAs *in vivo*.
⇒ Inactivation of the SPDEF programme in classical PDAs induces phenotype switching towards a basal-like differentiation.

HOW THIS STUDY MIGHT AFFECT RESEARCH, PRACTICE OR POLICY

⇒ The SPDEF-regulated enzymes AGR2 and *ERN2*/IREβ represent new therapeutic targets to investigate for the treatment of classical PDAs.
⇒ A comprehensive investigation of cell state interconversions during treatment may avoid relapse and improve overall responses in PDA patients.
⇒ Combination strategies that suppress distinct cell states may be required to overcome resistance.

INTRODUCTION

Pancreatic ductal adenocarcinoma (PDA) is a lethal cancer with a 5-year survival rate of only 12%.[1] The genetic drivers of PDA are well described: oncogenic KRAS mutations in the exocrine pancreas serve as an early event and promote the formation of precancerous lesions, including pancreatic intraepithelial neoplasia (PanIN) and intraductal papillary mucinous neoplasm (IPMN).[2] Subsequent inactivating mutations of tumour suppressor genes (eg, *TP53*, *CDKN2A*, *SMAD4*) drive tumour progression, a finding supported by genetically engineered mouse models (GEMMs) of PDA and genetic analysis of human tumour samples.[3 4] While the genetic progression of PDA is well characterised, the underlying molecular mechanisms are less understood.

Transcriptomic studies have revealed that PDAs can be clustered into two major subtypes, termed classical and basal-like.[5–8] PDAs of the classical subtype are typically lower grade tumours with a more favourable prognosis, whereas PDAs of the basal-like subtype are higher grade tumours associated with accelerated clinical progression. In addition, classical PDAs are well-differentiated and display glandular structures with high mucus-secreting activity, when compared with poorly differentiated basal-like PDAs with features of mesenchymal/squamous cells.[9] In accordance with the tumour histology, classical PDAs are enriched for the expression of endoderm specification genes, such as HNF1A, HNF4A and GATA6; whereas basal-like PDAs are characterised by the expression of genes involved in epithelial-to-mesenchymal transition (EMT), response to hypoxia and activation of the transcription factors (TFs) MYC and p63.[5–7] Subsequent studies have demonstrated that the phenotype of pancreatic cancer cells isn't fixed, but instead exists as dynamic cell states and that classical and basal-like phenotypes coexist within a single tumour and are the result of the integration of cell-intrinsic (eg, genomic aberrations, epigenetic factors) and cell-extrinsic (eg, microenvironmental changes, tissue architecture) inputs.[10–12] Additionally, intermediate coexpressor (IC) cells expressing genes of both subtypes have been identified in PDA, supporting the premise that PDA cells are plastic and interconvert between differentiation states.[13]

As phenotypic plasticity is now considered a new 'hallmark of cancer', the identification of the factors controlling intratumoral cell states is important for understanding the mechanisms of cancer initiation, progression and response to therapy for all neoplasms.[14] In this study, we reveal various pancreatic cancer differentiation states based on their gene expression profiles and identify a mucus production programme as a differentiation state-specific vulnerability for classical PDAs. Impairment of this programme diminished tumour expansion and shifted cells towards a more basal-like phenotype, indicating subtype switching as a cellular mechanism of resistance.

MATERIALS AND METHODS

Detailed methods are provided in the online supplemental materials and methods.

RESULTS

PDA samples reveal extensive intratumour heterogeneity

To unravel the transcriptional states underlying intratumour heterogeneity, we used the *Kras*$^{LSLG12D/+}$*; Trp53*$^{LSLR172H/+}$*; Pdx1-Cre* (KPC) GEMM in which Kras^{G12D} and p53^{R172H} were expressed in the pancreas under a Pdx1-Cre transgene.[15 16] KPC tumours are characterised by intratumour histological heterogeneity: areas of acinar-to-ductal metaplasia (ADM), low-grade and high-grade mPanINs are intermixed with invasive cancer cells.[15 16] We performed single-cell RNA sequencing (scRNA-seq) on ADM, mPanIN and neoplastic cells isolated by negative selection of stromal cells from 8 KPC tumours (online supplemental figure 1A; online supplemental table 1). Clustering of batch-adjusted, combined data of 23 991 cells identified six distinct expression states, with a similar contribution of cells from each tumour (online supplemental figure 1B,C). Three of the clusters were clearly demarcated: 'epithelial^{high}' cells in cluster 1 represented 22% of all cells and expressed high levels of epithelial markers and low levels of mesenchymal markers; mesenchymal cells in cluster 3 expressed genes associated with a mesenchymal differentiation and represented 12% of all cells; finally, proliferating cells in cluster 5 expressed genes encoding for proteins involved in cell cycle and mitosis and represented 5% of all cells (figure 1A, online supplemental figure 1D). In contrast, clusters 0, 2 and 4 expressed intermediate levels of epithelial and mesenchymal genes.

To reveal the evolutionary relationships and plasticity of these states, we ordered cells in pseudotime based on their transcriptional similarity. This unsupervised analysis ordered the cells on a V-shaped timeline and placed the epithelial^{high} cells at the bottom of the V and the mesenchymal and proliferating cells at the opposite ends of the trajectory (figure 1B). We next explored how expression states changed along the branches of the pseudotime trajectory. Epithelial^{high} cells in cluster 1 expressed high levels of epithelial markers and their expression was progressively lost or decreased along the pseudotime branches (figure 1C). Cells on the left branch of the pseudotime trajectory progressively acquired the expression of the master regulator of hypoxic signalling *Hif1a* and genes in the TGFβ pathway. Both Hif1α and TGFβ are known regulators of EMT.[17] Indeed, increased activation of Hif1α and the TGFβ pathway corresponded with increased expression of EMT genes and reached the highest expression in the mesenchymal cells in cluster 3.

Cells on the right branch of the pseudotime trajectory also lost or decreased the expression of epithelial genes and acquired the expression of the mesenchymal marker *Vim*. However, different from the cells on the left branch, cells on the right branch did not activate Hif1α or the TGFβ pathway and exhibited a partial EMT phenotype. Among these cells, the ones in cluster 5 expressed several genes involved in cell cycle, mitosis and nucleotide biosynthesis. Clusters 0, 2 and 4 reflected transition states between these phenotypes.

To localise these cell states spatially, we analysed the expression of a set of marker genes in tumour sections of KPCY mice (*Kras*$^{LSLG12D/+}$*; Trp53*$^{LSLR172H/+}$*; Pdx1-Cre; Rosa26*^{LSLYFP}), in which all pancreatic cells expressed yellow fluorescent protein (YFP).[18] In addition, to validate the temporal ordering of the pseudotime trajectory, KPCY tumours were immunolabeled for p53 and p19^{Arf}. The progression from precancerous lesions to invasive PDA in the KPC mouse model is associated with *Trp53* loss of heterozygosity (LOH).[15 19 20] p53 and p19^{Arf} stabilisation is characteristic of *Trp53* LOH cells, as shown by the protein expression analysis of organoids derived from KPC tumours (online supplemental figure 1E).[21] Furthermore, transcriptional analysis of the organoids identified the epithelial receptor *Fgfr2* as being highly expressed in KPC cells that retained the wild-type *Trp53* allele compared to *Trp53* LOH cells (online supplemental figure 1F). Investigation of the scRNA-seq data revealed *Fgfr2* expression in epithelial^{high} cells (online supplemental figure 1G).

Immunofluorescence labelling (IF) revealed the presence of epithelial^{high} cells expressing Fgfr2 and Epcam in glandular lesions comprised of cuboidal and columnar cells with histological features of ADM and mPanIN, but rarely in invasive cancer (figure 1D; online supplemental figure 1H). In agreement, Fgfr2-expressing cells infrequently exhibited markers of advanced disease, such as elevated expression of p53, p19^{Arf}, the DNA damage marker γH2AX and the proliferation marker Ki67 (online supplemental figure 1I–M). In contrast, mesenchymal cells marked by Zeb1 and Vimentin and proliferating cells marked by Ki67 and P-H3 displayed malignant histology and presented p53 and p19^{Arf} stabilisation.

Collectively, our data suggested that epithelial^{high} cells progressed to more aggressive phenotypes following inactivation of p53 by losing epithelial features while activating a partial or complete EMT programme. Therefore, targeting epithelial^{high} cells may block precancerous cells from evolving to invasive disease.

Consistent with others, our analysis found that PDA cells occupied a continuum of epithelial-to-mesenchymal expression

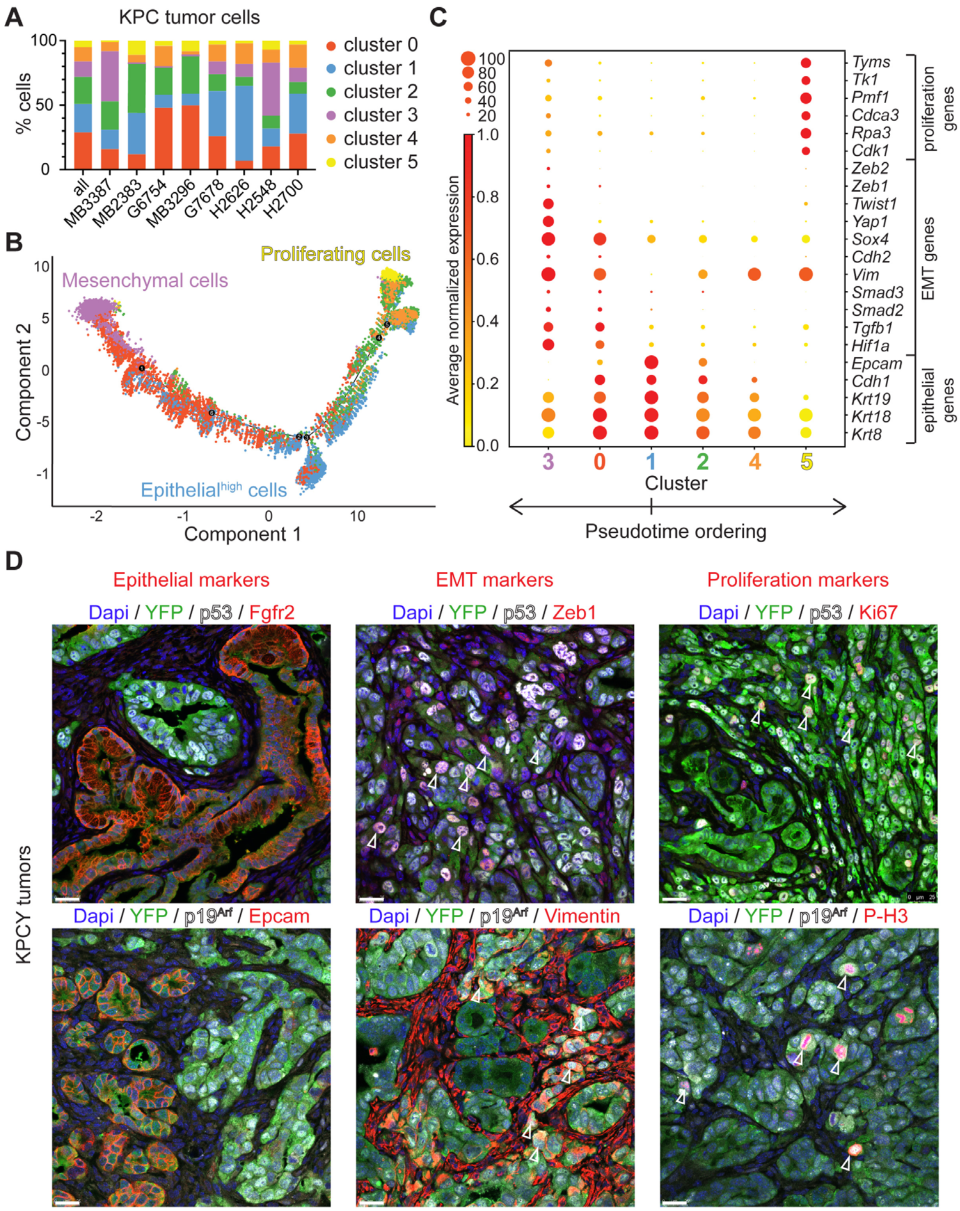

Figure 1 PDA samples reveal extensive intratumour heterogeneity. (A) Percentage of cells from eight independent KPC tumours present in each cluster. (B) Pseudotime ordering of KPC cells, colouring by cluster. (C) Dot plot of the expression of the indicated genes in the different clusters. The size of each dot represents the percentage of cells within a given cluster that expresses the gene; the intensity of colour indicates the average normalised expression. The order of the clusters matches the order of the clusters in the pseudotime trajectory. (D) Representative IF for YFP, p53 or p19^{Arf}, and Fgfr2, Epcam, Zeb1, Vimentin, Ki67, P-H3 in KPCY tumour sections. Scale bars, 25 µm. Arrow heads mark cells coexpressing p53 and Zeb1/Ki67 or p19^{Arf} and Vimentin/P-H3.

states, which defined the intratumour heterogeneity in KPC pancreatic tumours.[22 23]

Pancreatic precancerous lesions activate a secretory cell programme

Given that epithelial^{high} cells were enriched with precancerous cells, we sought to further investigate their biology and analysed the marker genes for cluster 1 (online supplemental figure 2A; online supplemental table 2). In addition to strong expression of epithelial genes, we found that epithelial^{high} cells upregulated genes associated with mucus production and secretion, including the TFs *Spdef* and *Foxa3* (figure 2A).

Spdef and Foxa3 are required for the differentiation of secretory cells, where they regulate mucus production, protein folding and glycosylation.[24–26] However, their role in pancreatic cancer progression remains unknown.

Although the mRNAs of some of these genes were barely detected by scRNA-seq, we showed by immunohistochemistry (IHC) that Spdef and Foxa3 target genes Agr2, Gcnt3, Clca1, Muc5ac,[24–26] the gastric genes Gkn2, Gkn3, Tff1, Tff2 and the epithelial markers Epcam and Fgfr2 were expressed by a large fraction of cells with precancerous histopathology in KPC tumour tissues (figure 2B,C). In addition, using RNA *in situ* hybridisation (RNA ISH) in combination with IF we demonstrated that *Spdef, Foxa3* and their target genes Agr2 and *Ern2* were often coexpressed with the epithelial^{high} cells markers Epcam and Gkn1 (figure 2D–G; online supplemental figure 2B,C). We selected Gkn1 because it was highly and selectively expressed by

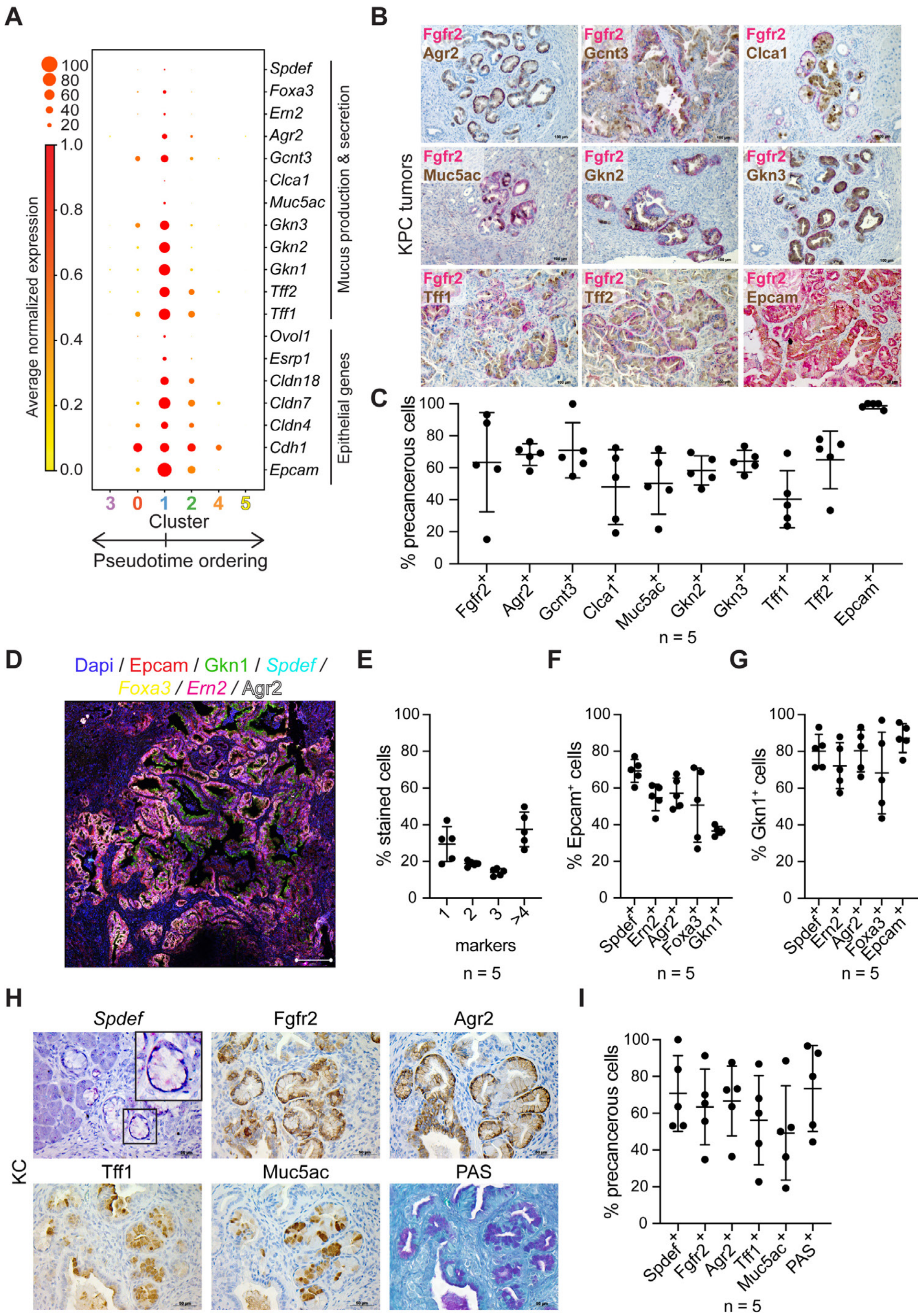

Figure 2 Pancreatic precancerous lesions activate a secretory cell programme. (A) Dot plot of the expression of the indicated genes in the different clusters. The size of each dot represents the percentage of cells within a given cluster that expresses the gene; the intensity of colour indicates the average normalised expression. The order of the clusters matches the order of the clusters in the pseudotime trajectory. (B) Representative IHC for Fgfr2 and Agr2, Gcnt3, Clca1, Muc5ac, Gkn2, Gkn3, Tff1, Tff2, Epcam in KPC tumour sections. (C) Average percentage±SD of precancerous cells expressing Fgfr2, Agr2, Gcnt3, Clca1, Muc5ac, Gkn2, Gkn3, Tff1, Tff2, Epcam in KPC tumour sections (n=5). (D) Representative RNA ISH of *Spdef, Foxa3* and *Ern2* combined with IF for Epcam, Gkn1 and Agr2 in a KPC tumour section. Scale bar, 200 µm. (E) Average percentage±SD of cells stained for one or more markers by RNA ISH combined with IF in KPC tumour sections (n=5). (F, G) Average percentage±SD of Epcam-positive (F) and Gkn1-positive (G) cells presenting the indicated markers in KPC tumour sections (n=5). (H) Representative RNA ISH of *Spdef,* IHC for Fgfr2, Agr2, Tff1, Muc5ac and PAS staining in pancreatic tissue from a 3 months-old KC mouse. Scale bars, 50 µm. (I) Average percentage±SD of precancerous cells expressing the indicated markers in pancreata from KC mice (n=5).

many, although not all, epithelial^{high} cells and Epcam because it was highly expressed by most epithelial^{high} cells and only weakly expressed by other cell states.

Next, to determine when these mucus-secreting cells first appeared during pancreatic tumourigenesis, we analysed the pancreata of *Kras*$^{LSLG12D/+}$; *Pdx1-Cre* (KC) mice for the expression of *Spdef* by RNA ISH, Fgfr2, Agr2, Tff1, Muc5ac by IHC and for the production of mucus by Periodic acid–Schiff (PAS) staining (figure 2H,I). We found that the expression of these genes and the secretion of mucus could be observed as early as transformation by $Kras^{G12D}$ initiated ADM and mPanIN development and persisted during disease progression in tumour-adjacent precancerous lesions. This mucus-producing programme was upregulated in precancerous cells as indicated by the analysis of published scRNA-seq datasets of mouse normal pancreas and premalignant lesions (online supplemental figure 2D,E).[27 28] Furthermore, although not activated following acute injury to the pancreas (online supplemental figure 2E), this programme was reported to be induced upon chronic injury.[29]

The repression of the Spdef programme in neoplastic cells was likely mediated by TGFβ signalling, a mechanism previously described in conjunctival epithelium.[30] Indeed, culturing of murine precancerous organoids in medium without any additives including the TGFβ inhibitor A83-01 ('Minimal' medium) resulted in the downregulation of *Spdef, Agr2* and *Ern2* (online supplemental figure 2F). The addition of TGFβ to the culture medium further reduced their expression and induced the expression of the mesenchymal genes *Vim* and *Zeb1*.

Spdef and its target genes *Ern2*/Ire1β and Agr2 support murine pancreatic tumour growth

Mucus production involves the complex folding and glycosylation of secreted proteins, including the high molecular weight mucins.[31] To investigate whether interfering with the regulation of mucus production would affect pancreatic cancer progression, we inactivated *Foxa3* and *Spdef* in mouse tumour organoids ('mT') using small guide RNA (sgRNA) pairs designed to delete the transcription start site (TSS) and isolated single-cell-derived clones. *Foxa3* and *Spdef* loss were assessed at the mRNA level, as we could not identify reliable antibodies (online supplemental figure 3A–E). The experiments on the effect of *Foxa3* deletion on the growth of mT69a and mT6 organoids *in vivo* did not demonstrate a dependency for tumour progression (online supplemental figure 3F,G). On the contrary, *Spdef* inactivation in two clones of mT69a severely impaired tumour growth *in vivo* following orthotopic transplantation (figure 3A; online supplemental figure 3H). In addition, mice transplanted with the slowest-growing clone showed significantly delayed PDA development (figure 3B). The tumour-promoting role of Spdef in pancreatic cancer progression was also confirmed in the tumour organoid line mT6 (figure 3C; online supplemental figure 3I). Notably, *Spdef* inactivation did not have a clear effect on tumour organoid proliferation *in vitro* and changes in duplication rate were minor and more likely due to clonality, suggesting an involvement of the pancreatic environment in determining Spdef-mediated tumour growth (online supplemental figure 3J).

To determine the molecular mechanism underlying the tumour growth defect observed upon *Spdef* loss, we performed genome-wide profiling of Spdef binding sites by Cleavage Under Targets & Release Using Nuclease (CUT&RUN) in KPC FC1245 cells expressing HA-tagged Spdef. We found that the majority of the high confidence peaks were located at promoters, introns and intergenic sites and enriched for the Spdef motif (figure 3D and E, online supplemental table 3). Next, we performed RNA sequencing (RNA-seq) of mT6 and mT69a organoid clones with or without knock-out (KO) of *Spdef* and restoration by cDNA expression (figure 3F; online supplemental table 4). We identified the Spdef-regulated genes whose differential expression upon *Spdef* deletion was reverted by Spdef re-expression. Of these genes, 5 were downregulated upon *Spdef* KO and upregulated upon its re-expression, while 11 were upregulated upon *Spdef* KO and downregulated upon its re-expression in both mT6 and mT69a organoids. The positively regulated genes were the TF *Foxa3*, the endoplasmic reticulum (ER)-resident disulfide isomerase *Agr2*, the secretory cells-specific ER stress sensor *Ern2*/Ire1β, the tight junction protein *Cldn2* and the cholesterol transporter *Gramd1b*. All of these genes presented a Spdef binding site in the CUT&RUN experiment.

Mucus-secreting cells rely on ER activity to achieve proper folding of secreted proteins and prevent ER stress.[32] As both Agr2 and *Ern2*/Ire1β are localised in the ER and play a role in the maintenance of ER homeostasis, we next investigated whether deletion of *Agr2* and *Ern2* would mimic the effect of deletion of *Spdef*.[33–35] We confirmed by RT-qPCR in mT6, mT23 and mT69a organoids that *Agr2* and *Ern2* were regulated by Spdef as previously reported (online supplemental figure 3K).[24 25] Furthermore, we verified Spdef-mediated modulation of Agr2 at the protein level too (figure 3G). *Agr2* and *Ern2* inactivation was achieved with sgRNA pairs designed to delete the TSS followed by the isolation of single-cell-derived clones. *Agr2* and *Ern2* loss were assessed at the mRNA level and by confirming the deletion of the TSS at the genomic DNA level (online supplemental figure 3L–N). We found that deletion of *Agr2* in two different mT69a clones reduced tumour growth *in vivo* following orthotopic transplantation (figure 3H; online supplemental figure 3O). Complete deletion of *Ern2* in mT69a and mT6 strongly impaired tumour growth *in vivo* (figure 3I,J; online supplemental figure 3P,Q). Of note, partial inactivation of *Ern2* in mT69a had an intermediate effect. Thus, similar to Spdef, *Ern2*/Ire1β and Agr2 promoted the growth *in vivo* of epithelial pancreatic cancer cells.

The tumours formed following mT organoid implantation were highly cellular and did not produce mucus, independently of whether they were derived from mT organoids expressing or not *Spdef, Agr2* or *Ern2* (online supplemental figure 3H,I, O–Q). We analysed *Spdef* and *Ern2* expression by RNA ISH and Agr2 expression by IHC and found that most of the malignant cells in control tumours did not express *Spdef*, *Ern2* or Agr2 except for few rare lesions (online supplemental figure 3R). We concluded that Spdef, *Ern2*/Ire1β and Agr2 were required in the early events of tumourigenesis before tumour cells lost their epithelial and mucus-secreting nature and underwent malignant differentiation to more invasive phenotypes, in accordance with the tumour progression model inferred from the analysis of the scRNA-seq data.

The SPDEF-regulated mucus production programme is expressed by human precancerous lesions and classical PDAs

To determine whether mouse PDAs have similar expression states to human PDAs or vice versa, we performed a comparative analysis of cell differentiation states between mice and humans. Human PDA expression states derived from scRNA-seq were defined as scClassical, IC and scBasal.[13] To this end, we calculated scores based on the expression of mouse and human PDA signatures in single KPC tumour cells and human PDA cells (figure 4A; online supplemental table 5).[13] Notably, pairwise comparisons of the expression of our mouse PDA signatures with murine versions of the human PDA signatures revealed that expression of the $epithelial^{high}$ cell signature was strongly correlated with the expression of the scClassical signature (R=0.87) in single KPC tumour cells (figure 4A—left panel; online supplemental figure 4A). However, murine correlates of the human IC and scBasal states were less apparent. Next, we evaluated the reciprocal relationships by analysing the expression of humanised versions of the mouse PDA signatures in single human PDA cells (figure 4A—right panel). We found that expression of the $epithelial^{high}$ cells signature strongly correlated with expression of the scClassical

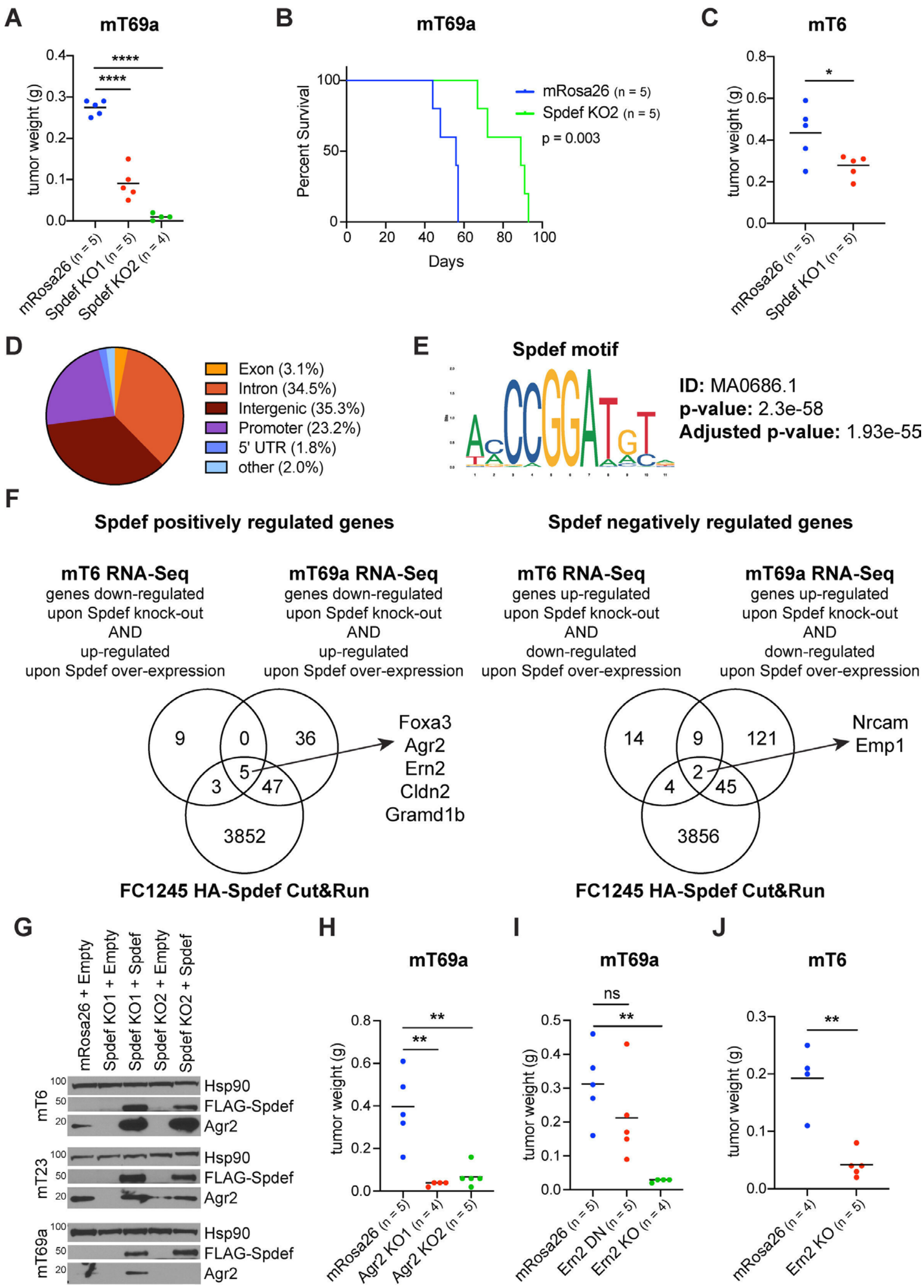

Figure 3 Spdef and its target genes *Ern2*/Ire1β and Agr2 support murine pancreatic tumour growth. (A, C, H, I, J) Quantification of weight of tumours derived from mT69a (A, H, I) and mT6 (C, J) orthotopically grafted organoid (OGO) models of *Spdef* KO (A, C), *Agr2* KO (H), *Ern2* KO or partial inactivation DN (I, J) and mRosa26 clones in nu/nu mice. Results show mean of biological replicates. Unpaired Student's t-test. (B) Kaplan-Meier survival curve of percent survival for mT69a OGO models of *Spdef* KO and mRosa26 clones in nu/nu mice. Log-rank (Mantel-Cox) test. (D) Pie chart of percent distribution of high confidence HA-Spdef peaks (≥2 replicates) across genomic features. (E) Spdef motif enrichment as determined by MEME motif analysis on the high confidence HA-Spdef-binding sites. (F) Venn diagram of the differentially expressed genes identified by RNA-seq following *Spdef* KO and restoration by cDNA expression in mT69a and mT6 organoids (upregulated genes: q-value<0.05, $\log_2$ of fold change>0; downregulated genes: q-value<0.05, $\log_2$ of fold change<0). Genes assigned to HA-Spdef peaks in KPC FC1245 cells are indicated. (G) Agr2 and FLAG-Spdef expression analysis by Western blotting in mT6, mT23 and mT69a organoids following *Spdef* KO and restoration by cDNA expression. Loading control: Hsp90.

signature (R=0.83), poorly correlated with expression of the IC signature (R=0.19) and inversely correlated with expression of the scBasal signature (R=−0.43) (online supplemental figure 4A). In addition, expression of the mesenchymal cancer cells signature moderately correlated with expression of the scBasal signature (R=0.38) and inversely correlated with expression of the scClassical signature (R=−0.34). Taken together, this analysis revealed high correlation between murine epithelial^{high} cells and human classical PDA cells expression states. This result was consistent with the previous findings that classical PDAs exhibited the epithelial and mucus-secreting nature displayed in KPC precancerous cells.[6]

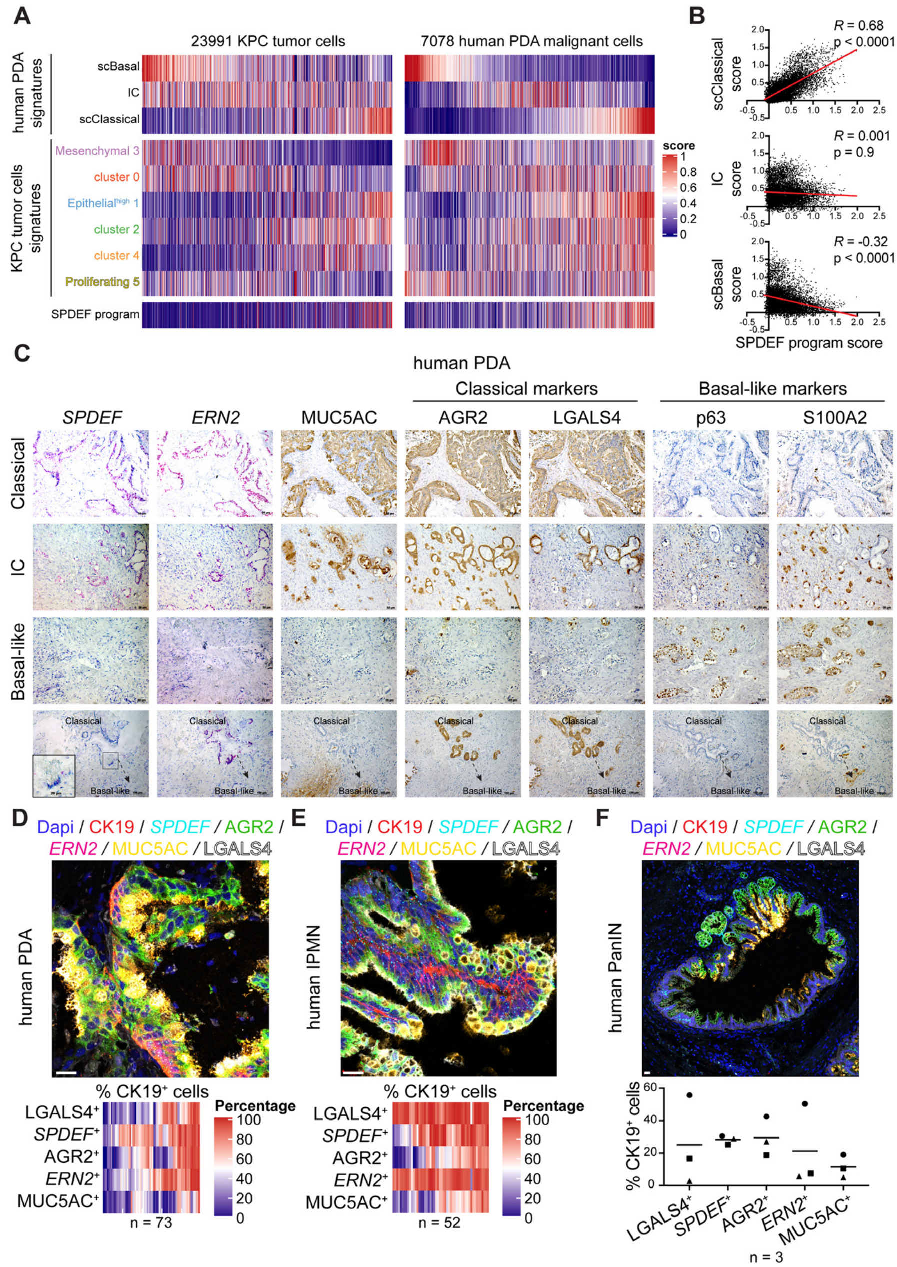

Figure 4 The SPDEF-regulated mucus production programme is expressed by human precancerous lesions and classical PDAs (A) Heatmap of signature scores (rows) in single KPC tumour cells and human PDA malignant cells (columns).[13] (B) Correlation between SPDEF programme score (x-axis) and signature scores (y-axis) in single human PDA malignant cells.[13] Spearman's rank correlation coefficient and p value. (C) Representative RNA ISH of *SPDEF* and *ERN2* and IHC for MUC5AC, AGR2, LGALS4, p63, S100A2 in serial sections of human PDAs of classical, IC and basal-like differentiation. (D–F) Representative RNA ISH of *SPDEF* and *ERN2* combined with IF for CK19, AGR2, MUC5AC and LGALS4 in a human PDA TMA (n=73) (D) a human IPMN TMA (n=52) (E) and human PanINs (n=3) (F) Scale bar, 200 µm. The percentage of CK19-positive cells presenting the indicated markers is reported.

Next, we sought to compare the expression of the SPDEF programme with human and mouse PDA signatures, respectively (figure 4A,B; online supplemental figure 4A). We found a strong correlation with the expression of the scClassical signature ($R=0.68$), a poor correlation with the expression of the IC signature ($R=0.0001$) and an inverse correlation with the expression of the scBasal signature ($R=-0.32$). To corroborate this finding, we analysed RNA-seq data of laser-capture microdissected epithelium from patients with PDA and our models of intraductally grafted slow and fast-progressing human organoid lines, which recapitulated the features of the classical and basal-like differentiation of human PDA, respectively (online supplemental figure 4B–D).[10 12 36] We established that classical PDAs and slow progressors presented a significantly higher expression of the SPDEF programme compared to basal-like PDAs and fast progressors, suggesting that the SPDEF programme may be vital for classical differentiation.

Since in the KPC GEMM the Spdef programme was highly expressed in precancerous cells that retained the wild-type *Trp53* allele, we evaluated whether the *TP53* status correlated with the expression of the SPDEF programme in human PDAs but did not observe any significant association (online supplemental figure 4E–G). On the contrary, in two out of three of the datasets we analysed, we found a statistically significant increase in the expression of the SPDEF programme in SMAD4 altered compared with wild-type human PDAs, further supporting a role for TGFβ signalling in inhibiting SPDEF activation (online supplemental figure 4H–J).

To validate our findings from these *in silico* analyses, we evaluated the expression of *SPDEF* and *ERN2* by RNA ISH and AGR2 and MUC5AC by IHC in human PDAs of classical, IC and basal-like differentiation, as defined by p63, S100A2 and LGALS4 immunolabeling (figure 4C). Of note, AGR2 is also a classical marker.[6] We confirmed that *SPDEF* and its targets were highly expressed in classical PDAs, moderately expressed in IC PDAs and absent or only weakly expressed in basal-like PDAs. This expression pattern was particularly evident in a PDA sample in which classical PDA cells were located adjacent to basal-like PDA cells. Next, we extended this analysis by performing RNA ISH in combination with IF on a tissue microarray (TMA) of PDA samples and verified that PDAs with a high percentage of malignant cells expressing the classical marker LGALS4 presented a high percentage of *SPDEF, ERN2,* AGR2 and MUC5AC expressing cells (figure 4D; online supplemental figure 4K).

Recently, other groups reported that PanIN lesions exhibited a classical differentiation and that SPDEF was activated as indolent IPMNs progressed to higher-grade lesions.[37–39] Here, we revealed by RNA ISH combined with IF that *SPDEF* and its target genes *ERN2*, AGR2 and MUC5AC were expressed in IPMNs of the pancreas and human PanINs (figure 4E and F; online supplemental figure 4L).

Finally, we evaluated previously published transcriptome data comparing normal human pancreas and PDA and found that *SPDEF* was upregulated in tumour and metastatic lesions (online supplemental figure 4M).[6] We further corroborated the increased expression pattern of *SPDEF* in organoid cultures derived from human PDA tumours, while *SPDEF* was expressed at low levels in organoids derived from normal pancreatic epithelial cells (online supplemental figure 4N).[40]

Collectively, we found that the expression of SPDEF was elevated in human precancerous lesions and classical PDAs, reduced in IC PDAs and repressed in basal-like PDAs, revealing a potential role of SPDEF in the transitions of cell differentiation states during PDA progression.

Classical PDAs are dependent on SPDEF for tumour growth

We next sought to understand the function of SPDEF in human PDA progression. First, we assessed *SPDEF* expression in several non-primary PDA cell lines and the slow-progressing human organoid line hF27, which were defined as classical or basal-like by transcriptomic analyses not always in agreement (online supplemental figure 5A).[12 41–43] Intriguingly, we found that *SPDEF* mRNA levels correlated with the molecular subtype of the PDA cells *in vivo*, but that was not the case *in vitro* (figure 5A,B; online supplemental figure 5B). Following orthotopic transplantation into NOD scid gamma (NSG) mice, the PDA cells separated into two groups: high SPDEF-expressing tumours (hF27, CFPAC1 and HPAF-II) and low SPDEF-expressing tumours (BxPC3, YAPC and AsPC1). The high SPDEF-expressing tumours were well differentiated and expressed the TF determinants of classical differentiation FOXA1, GATA6 and HNF4A. Conversely, the low SPDEF-expressing tumours were poorly differentiated and expressed known TF drivers of basal-like differentiation: BxPC3 and YAPC tumours activated p63, while AsPC1 tumours ZEB1.[17 41] Thus, we confirmed that SPDEF is highly expressed by classical PDAs and absent or only weakly expressed by basal-like PDAs.

To determine if SPDEF supports the growth of classical PDA, we deleted *SPDEF* in high SPDEF-expressing PDA cell lines using sgRNA pairs designed to eliminate the TSS and isolated single-cell-derived clones (online supplemental figure 5C,D). *SPDEF* loss did not slow the rate of cell division *in vitro* (online supplemental figure 5E); however, it severely impaired the growth of hF27, CFPAC1 and HPAF-II tumours *in vivo* following orthotopic transplantation and it extended the survival of orthotopically grafted HPAF-II tumour models (figure 5C–G; online supplemental figure 5F–I). Of note, the growth defect *in vivo* of CFPAC1 and HPAF-II *SPDEF* KO cells could only be partially rescued when the *SPDEF* cDNA was introduced before performing the inactivation of the endogenous gene.

Next, to determine the effect of *SPDEF* on the growth of basal-like tumours, we performed loss-of-function and gain-of-function experiments (online supplemental figure 5J). We found that genetic manipulation of *SPDEF* in BxPC3, YAPC and AsPC1 cells did not have a clear effect on the proliferation *in vitro* (online supplemental figure 5K). In addition, it did not alter tumour growth *in vivo* for BxPC3 and YAPC cells or extend the survival of orthotopically grafted AsPC1 tumour models (figure 5H–J; online supplemental figure 5L,M).

To investigate the molecular mechanisms underlying the impaired growth of *SPDEF* KO classical PDAs, we performed RNA-seq on the xenografts. Consistent with the slower growth *in vivo*, we observed the repression of proliferation-related genes in *SPDEF*-deleted tumours (figure 5K–M; online supplemental table 6).

Altogether, our results strongly indicated that SPDEF was important for the growth of classical PDAs.

The SPDEF target genes *ERN2*/IRE1β and AGR2 support classical PDA growth and prevent aberrant mucus production

PDA precancerous lesions and classical PDAs were associated with high levels of mucins in histopathological assessment.[2 6] Given the finding that SPDEF was highly active in these cells, we investigated SPDEF's role in the regulation of mucus production.

First, we explored whether genetic manipulation of *SPDEF* would affect the mucus-secreting activity of classical and basal-like tumours by Alcian blue (AB) staining. We found that deletion of *SPDEF* reduced mucus secretion in BxPC3 and YAPC tumour models and *SPDEF* overexpression partially restored mucus production in YAPC tumours, while it significantly induced mucus production in BxPC3 tumours (figure 6A,B). The rescue in mucus production correlated with the restoration in the expression of SPDEF target genes *AGR2, ERN2* and *MUC5AC* which was complete in BxPC3 tumours and only partial in YAPC tumours (figure 6D). AsPC1 control tumours were unique as they presented the lowest expression of *SPDEF* and did not secrete mucus (figures 5A and 6C). In these tumours, SPDEF overexpression induced the upregulation of SPDEF target genes and TFF1, a peptide found in mucus (figure 6C,D). In AsPC1 tumours, mucus production was assessed by TFF1 IHC as necrotic areas confounded the quantification. In summary, SPDEF modulated mucus production in basal-like tumours.

Next, we further characterised classical tumours. To our surprise, we did not observe any alteration in mucus

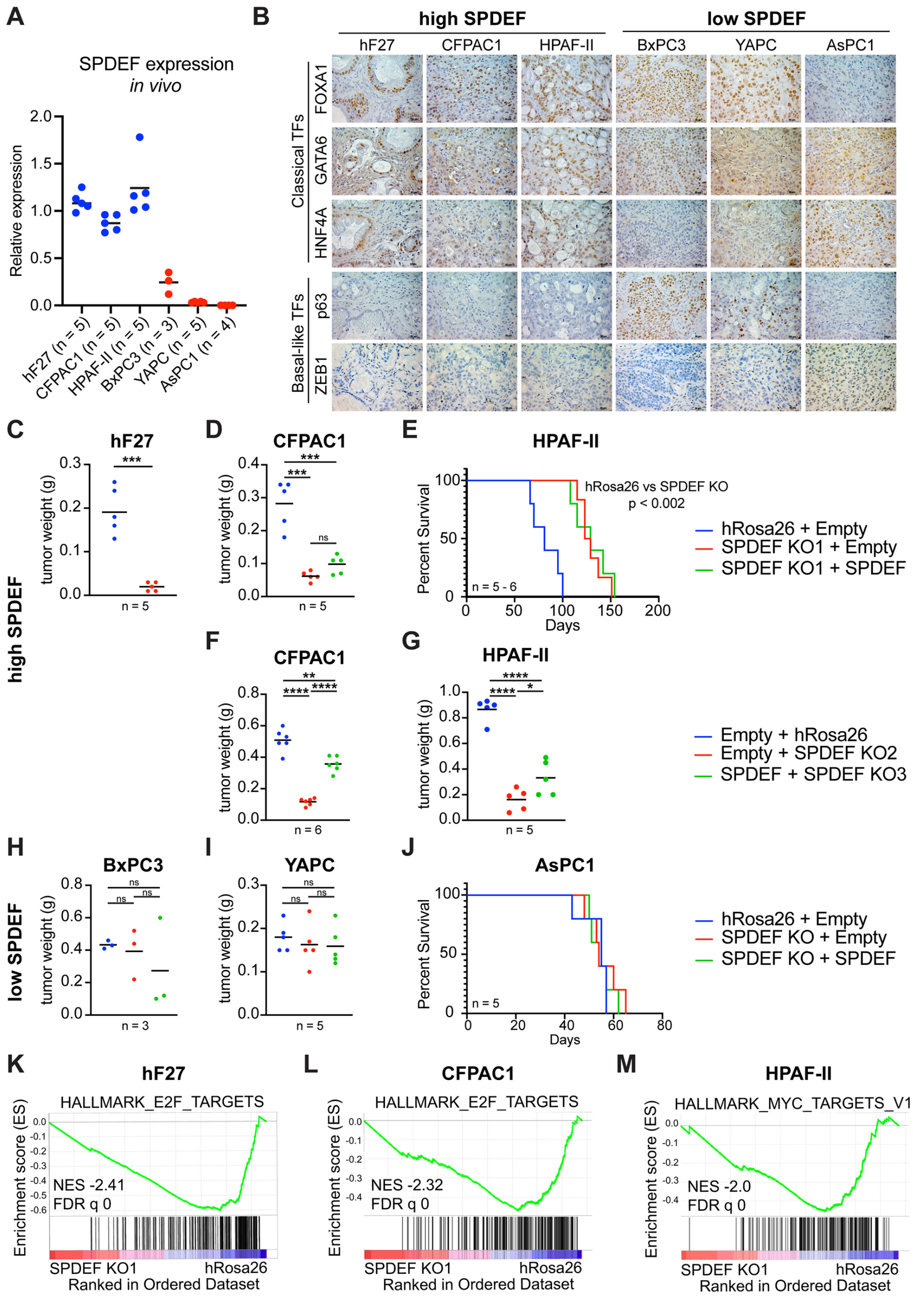

Figure 5 Classical PDAs are dependent on SPDEF for tumour growth. (A) RT-qPCR analysis of *SPDEF* expression in control tumours derived from transplant models of hF27, CFPAC1, HPAF-II, BxPC3, YAPC and AsPC1. Results show mean of biological replicates. (B) Representative IHC for FOXA1, GATA6, HNF4A, p63 and ZEB1 in control tumours derived from transplant models of hF27, CFPAC1, HPAF-II, BxPC3, YAPC and AsPC1. (C) Quantification of weight of tumours derived from hF27 orthotopically grafted models of *SPDEF* KO and hRosa26 clones in NSG mice. Results show mean of biological replicates. Unpaired Student's t-test. (D, H, I) Quantification of weight of tumours derived from CFPAC1 (D), BxPC3 (H) and YAPC (I) orthotopically grafted models of hRosa26 and *SPDEF* KO clones with (SPDEF) or without (Empty) *SPDEF* cDNA expression following the knock-out in NSG mice. Results show mean of biological replicates. Unpaired Student's t-test. (E, J) Kaplan-Meier survival curve of per cent survival for HPAF-II (E) and AsPC1 (J) orthotopically grafted models of hRosa26 and *SPDEF* KO clones with (SPDEF) or without (Empty) *SPDEF* cDNA expression following the knock-out in NSG mice. Log-rank (Mantel-Cox) test. (F, G) Quantification of weight of tumours derived from CFPAC1 (F) and HPAF-II (G) orthotopically grafted models of hRosa26 and *SPDEF* KO clones with (SPDEF) or without (Empty) *SPDEF* cDNA expression prior to the knock-out in NSG mice. Results show mean of biological replicates. Unpaired Student's t-test. (K, L) GSEA signature 'HALLMARK_E2F_TARGETS' is repressed in hF27 and CFPAC1 *SPDEF* KO1 compared to hRosa26 tumours. (M) GSEA signature 'HALLMARK_MYC_TARGETS_V1' is repressed in HPAF-II *SPDEF* KO1 compared with hRosa26 tumours. NES, normalised enrichment score; FDR, false discovery rate.

production in *SPDEF* KO tumours by AB staining and IF for MUC5AC (online supplemental figure 6A,B). The TF MYRF was previously reported to protect classical PDA cells from ER stress caused by mucus production by regulating genes involved in protein maturation and the unfolded protein response (UPR).[44] We wondered whether MYRF or other UPR genes could be compensating for the loss of *SPDEF*; however, we found that their expression was not increased in *SPDEF* KO tumours (online supplemental figure 6C). Furthermore, differently from *MYRF* KO cells, *SPDEF* KO

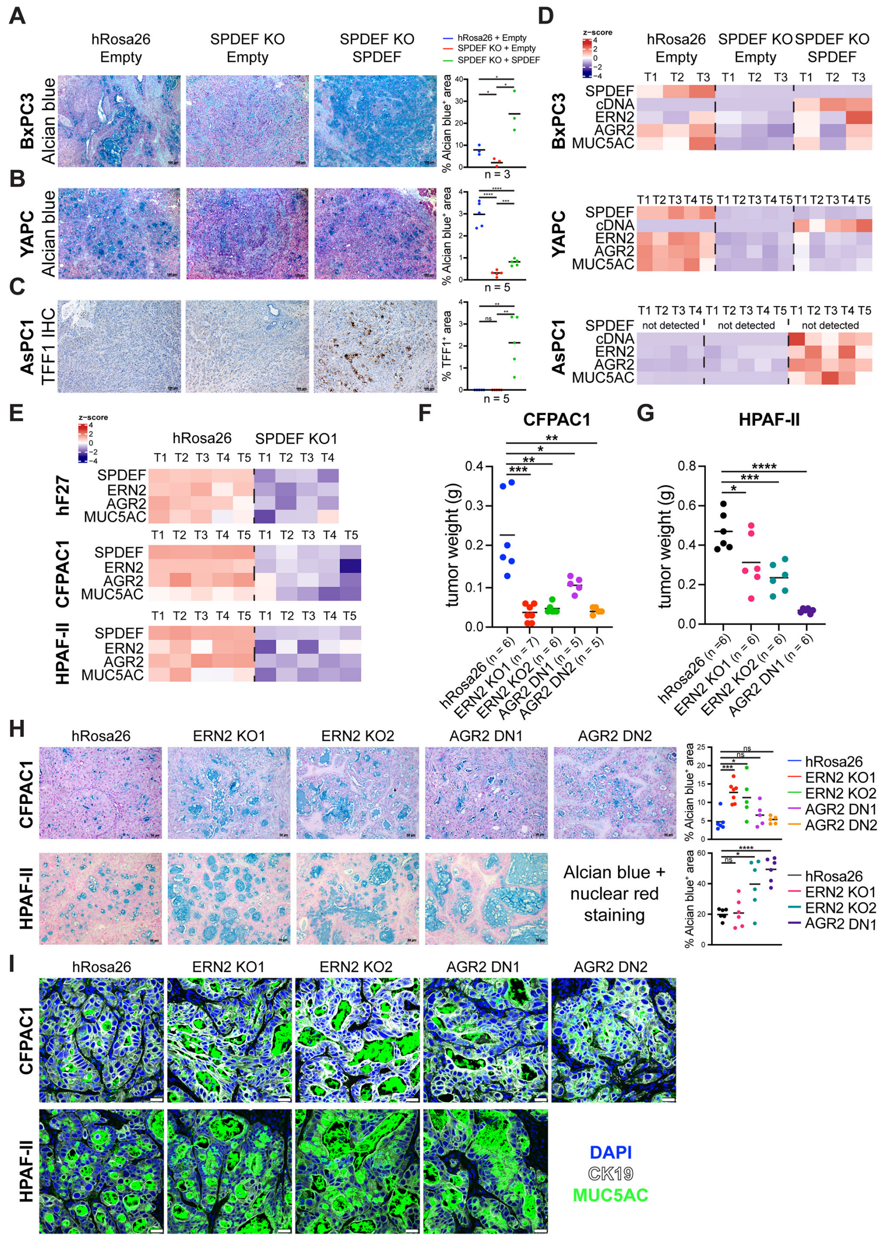

Figure 6 The SPDEF target genes *ERN2*/IRE1β and AGR2 support classical PDA growth and prevent aberrant mucus production (A, B) Left, representative AB and nuclear red staining of BxPC3 and YAPC orthotopically grafted models of hRosa26 and *SPDEF* KO clones with (SPDEF) or without (Empty) *SPDEF* cDNA expression. Scale bars, 100 µm. Right, average percentage of AB positive area. Unpaired Student's t-test. (C) Left, representative IHC for TFF1 in AsPC1 orthotopically grafted models of hRosa26 and *SPDEF* KO clones with (SPDEF) or without (Empty) *SPDEF* cDNA expression. Scale bars, 100 µm. Right, average percentage of TFF1 positive area. Unpaired Student's t-test. (D) Heatmap of z-score values of *SPDEF, SPDEF* cDNA, *ERN2, AGR2* and *MUC5AC* expression as determined by RT-qPCR in tumours derived from BxPC3, YAPC and AsPC1 orthotopically grafted models of hRosa26 and *SPDEF* KO clones with (SPDEF) or without (Empty) *SPDEF* cDNA expression. (E) Heatmap of z-score values of *SPDEF, ERN2, AGR2* and *MUC5AC* expression as determined by RNA-seq in tumours derived from hF27, CFPAC1 and HPAF-II orthotopically grafted models of *SPDEF* KO1 and hRosa26 clones. (F, G.) Quantification of weight of tumours derived from CFPAC1 (F) and HPAF-II (G) orthotopically grafted models of *ERN2* KO, *AGR2* partial inactivation DN and hRosa26 clones in NSG mice. Results show mean of biological replicates. Unpaired Student's t-test. (H) Left, representative AB and nuclear red staining of CFPAC1 and HPAF-II orthotopically grafted models of *ERN2* KO, *AGR2* partial inactivation DN and hRosa26 clones. Scale bars, 100 µm. Right, average percentage of AB positive area. Unpaired Student's t-test. (I) Representative IF for CK19 and MUC5AC in tumour sections derived from CFPAC1 and HPAF-II orthotopically grafted models of *ERN2* KO, *AGR2* partial inactivation DN and hRosa26 clones. Scale bars, 25 µm.

cells were as sensitive as control cells to ER stress-inducing drugs Thapsigargin, Tunicamycin and Brefeldin A (online supplemental figure 6D).

Next, we hypothesised that the tumours might have reacquired expression of *SPDEF* or its target genes. However, we confirmed *SPDEF* inactivation by RNA-seq on the tumours' RNA (figure 6E; online supplemental table 6). Furthermore, we showed that SPDEF target genes *AGR2*, *ERN2* and *MUC5AC* were downregulated at the mRNA level in *SPDEF* KO tumours. However, this transcriptional repression was only partial. Analysis of published ChIP-seq data in CFPAC1 cells and CUT&RUN profiling of GATA6 binding sites in HPAF-II cells indicated that the expression of *AGR2, ERN2* and *MUC5AC* was potentially regulated by additional TFs controlling classical differentiation in PDA which may compensate for the loss of SPDEF (online supplemental figure 6E, online supplemental table 3).[42]

To investigate whether the residual expression of *ERN2*/IRE1β and AGR2 in *SPDEF* KO tumours could explain the lack of measurable alterations in mucus production, we deleted *ERN2* and *AGR2* in CFPAC1 and HPAF-II cells using sgRNA pairs designed to eliminate the TSS and isolated single-cell-derived clones (online supplemental figure 6F,G). We were able to KO *ERN2* but only partially inactivate *AGR2* as assessed at the mRNA level and by measuring the deletion of the TSS by PCR on the genomic DNA. Inactivation of *ERN2* and *AGR2* did not have a clear effect on cell proliferation *in vitro*; however, it severely impaired tumour growth *in vivo* following orthotopic transplantation (figure 6F,G; online supplemental figure 6H–J). Analysis of mucus production by AB staining indicated that *ERN2* deletion resulted in enlarged ducts associated with aberrant mucus accumulation, which was reminiscent of the phenotype observed in *MYRF* KO tumours (figure 6H).[44] Partial inactivation of *AGR2* also resulted in an abnormal increase in secreted mucus in HPAF-II tumours, but not in CFPAC1 tumours. CFPAC1 *AGR2* inactivated tumours presented abnormally high levels of MUC5AC intracellularly as shown by IF (figure 6I).

Overall, these data indicated that SPDEF controlled *ERN2*/IRE1β and AGR2 expression, which in turn regulated mucus production and secretion.

Inactivation of the SPDEF-regulated mucus production programme was associated with features of classical-to-basal-like phenotype switch

Expression analysis of CFPAC1 and HPAF-II tumours revealed downregulation of classical genes and upregulation of basal-like genes in *SPDEF* KO compared to control tumours (figure 7A,B; online supplemental table 6). This suggested that *SPDEF* KO cells were under selective pressure to undergo phenotypic interconversion to survive and grow. Specifically, in CFPAC1 tumours we noted the activation of a squamous differentiation programme as indicated by the statistically significant upregulation of *TP63* and its target gene *KRT5*, while in HPAF-II tumours we observed the activation of an EMT programme as indicated by the statistically significant induction of the EMT regulator *ALX1* and the basal-like marker *KRT81* (online supplemental figure 7A,B).[41 45 46] Immunolabeling analysis showed that many cells in CFPAC1 tumours activated p63 and its target gene S100A2, while some cells in HPAF-II tumours induced the EMT regulator SLUG following *SPDEF* inactivation (figure 7C,D; online supplemental figure 7C).[17] Of note, the phenotypic interconversion could be prevented when the *SPDEF* cDNA was introduced before performing the KO of the endogenous gene, suggesting that SPDEF loss irreversibly committed PDA cells to certain differentiation fates.

We next investigated *ERN2*- and *AGR2*-inactivated tumours. We found that, same as *SPDEF* KO tumours, CFPAC1 tumours inactivated for *ERN2* and *AGR2* increased the expression of p63 and S100A2, while HPAF-II tumours SLUG (figure 7E; online supplemental figure 7D). Notably, p63, S100A2 and SLUG upregulation were not observed *in vitro* preimplantation, suggesting an involvement of the microenvironment in driving the phenotypic interconversion (online supplemental figure 7E–G).

In sum, SPDEF and its target genes *ERN2*/IRE1β and AGR2 supported the fitness of classical PDAs. In response to their abrogation, tumours initiated a classical-to-basal-like phenotype switch.

DISCUSSION

PDA is a heterogeneous disease as a result of cell plasticity.[10 11 13] Identifying the determinants of cancer cell plasticity is crucial to comprehend disease progression and develop optimal treatment strategies. Here, we identified multiple expression states in a well-established GEMM of pancreatic cancer that reflected different stages of the disease, and revealed some of the TFs driving these phenotypes. In addition, we described a previously unappreciated role for Spdef, the master regulator of secretory cell development, in promoting pancreatic cancer.

We discovered that Spdef was expressed in precancerous lesions and then its expression was repressed as neoplastic cells became invasive by TGFβ signalling. By comparative analysis of cell differentiation states in mice and humans, we found that the expression of the SPDEF programme was elevated in human precancerous lesions and classical PDAs and reduced in basal-like PDAs. Loss of SPDEF and its target genes *AGR2* and *ERN2*/IRE1β impaired the growth of mouse tumour organoids and classical PDA cells *in vivo*.

SPDEF was reported to exhibit both tumour-suppressive and oncogenic functions. Our current understanding of SPDEF's role in supporting PDA cells with epithelial/classical but not invasive/basal-like phenotype could help to reconcile some of these controversial findings. For example, SPDEF induced mammary luminal epithelial lineage-specific gene expression and promoted the survival of luminal tumour cells.[47] On the contrary, expression of SPDEF inhibited growth, motility and invasion of aggressive basal breast cancer cell lines.[48 49] Similar to breast cancer cells, SPDEF promoted luminal epithelial differentiation in prostate cancer and deletion of SPDEF in luminal cells resulted in the induction of EMT-related proteins and increased migration while expression of SPDEF in invasive cells suppressed metastasis formation by inducing epithelial features.[50–52] By analysing both the classical and basal-like phenotypes of PDA, we revealed that SPDEF is a mediator of epithelial/classical identity and its activity is dependent on the cell differentiation state. Furthermore, SPDEF's role as a mediator of classical identity was needed to optimally support tumour growth, as indicated by the finding that the growth defect induced by SPDEF loss in classical PDAs could be partially rescued only when *SPDEF* cDNA expression was introduced before knocking-out the endogenous gene. In addition, *SPDEF* loss facilitated subtype interconversion from a classical towards a basal-like differentiation, which was reminiscent of the phenotype switch induced by inactivation of the TF determinants of classical differentiation FOXA1 and FOXA2 in lung cancer and GATA6, HNF1 and HNF4 in PDA.[53 54]

Mucin production plays an important role in the biology of normal and diseased pancreas.[31] Here, we found that Spdef was expressed by mucus-secreting precancerous lesions in KPC tumours. In human PDA, SPDEF was sufficient but not necessary to regulate mucus production. Indeed, genetic manipulation of SPDEF modulated mucus production in basal-like tumours. Meanwhile, deletion of SPDEF in classical tumours did not ablate their secretory function. Altogether, this indicated that SPDEF is one but not the only regulator of mucus production in PDA.

Mucus-secreting cells must adapt the activity of their ER to sustain the complex folding and glycosylation of secreted proteins.[32] One of the strategies adopted by mucus-producing PDAs to deal with the stress caused by mucus production, is

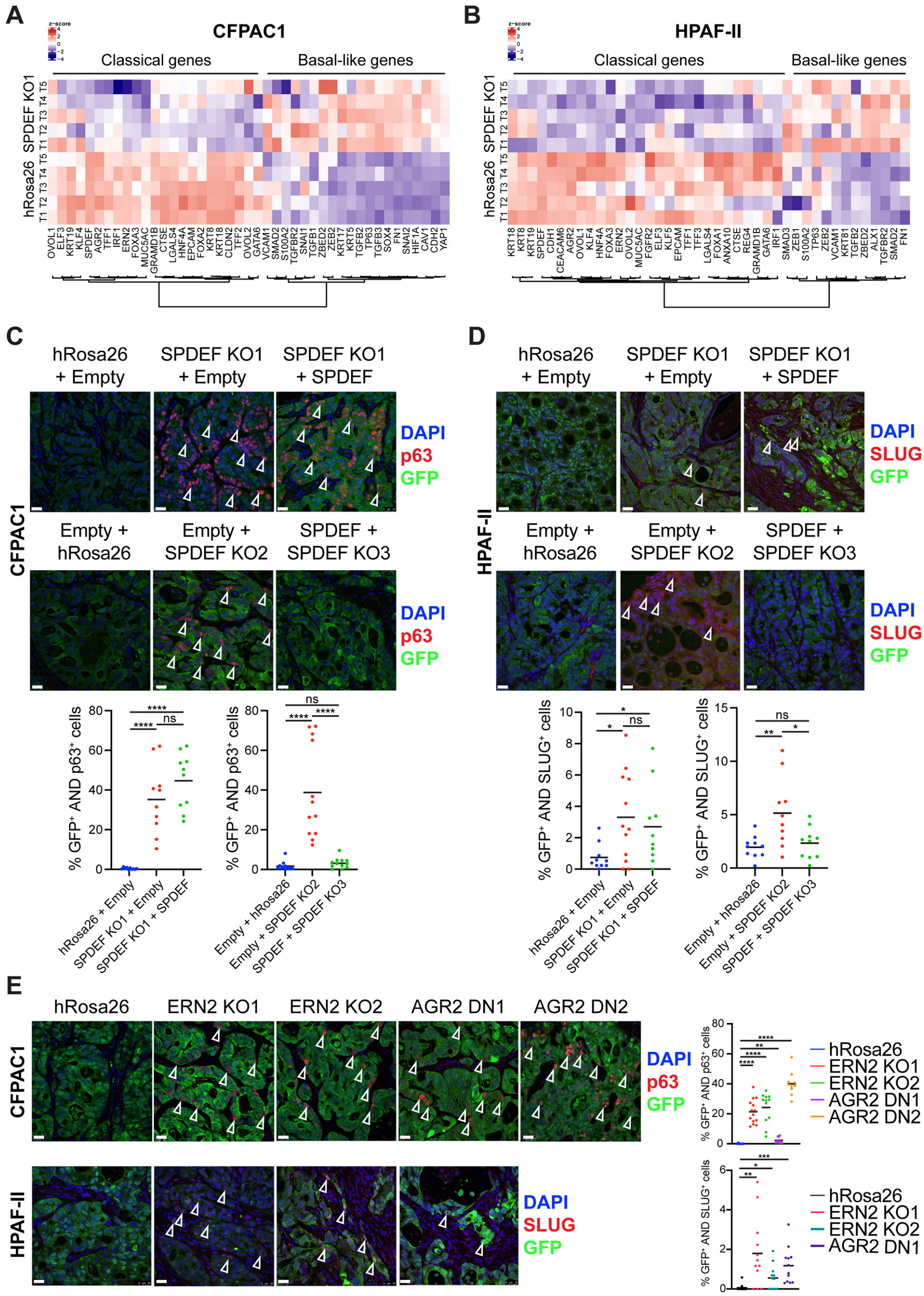

Figure 7 Inactivation of the SPDEF-regulated mucus production programme was associated with features of classical-to-basal-like phenotype switch. (A, B) Heatmap of z-score values of the expression for the indicated genes as determined by RNA-seq in tumours derived from CFPAC1 (A) and HPAF-II (B) orthotopically grafted models of *SPDEF* KO1 and hRosa26 clones. (C) Top, representative IF for GFP and p63 in CFPAC1 hRosa26 and *SPDEF* KO tumours with *SPDEF* cDNA expression after or prior the knock-out as indicated. Scale bars, 25 µm. Bottom, average percentage of GFP- and p63-expressing cells. Two images per tumour were quantified. Unpaired Student's t-test. (D) Top, representative IF for GFP and SLUG in HPAF-II hRosa26 and *SPDEF* KO tumours with *SPDEF* cDNA expression after or prior the knock-out as indicated. Scale bars, 25 µm. Bottom, average percentage of GFP- and SLUG-expressing cells. Two images per tumour were quantified. Unpaired Student's t-test. (E.) Left, representative IF for GFP and p63 or SLUG in CFPAC1 and HPAF-II hRosa26, *ERN2* KO and *AGR2* partial inactivation DN tumour sections as indicated. Scale bars, 25 µm. Right, average percentage of GFP- and p63- or SLUG-expressing cells. Two images per tumour were quantified. Unpaired Student's t-test.

represented by the activation of the TF MYRF, which maintains ER integrity and prevents ER stress by regulating genes involved in protein maturation and the UPR.[44] Here, we found that Spdef supported PDA growth by inducing the ER-resident disulfide isomerase Agr2 and secretory cell-specific ER stress sensor *Ern2*/Ire1β. Collectively, our results established a new oncogenic role for Spdef in pancreatic cancer and indicated that mucus-secreting neoplastic cells hijacked the physiological function of this TF to promote ER homoeostasis and tumourigenesis. Our data supported and extended the previous discovery that Agr2 was induced in response to ER stress and required for the initiation of pancreatic cancer.[55] Here, we demonstrated that Agr2 was regulated by Spdef and supported tumourigenesis by preventing aberrant mucus production. In addition, our study identified a role for *Ern2*/Ire1β in tumourigenesis. In goblet cells and airway epithelium, *Ern2*/Ire1β, but not its most studied paralog and mediator of UPR *Ern1*/Ire1α, promoted efficient mucin production and folding in the ER.[56–59] Our work indicated that the distinctive role of *Ern2*/Ire1β in preventing ER stress caused by the folding of mucins and other secreted proteins had a tumour-promoting role in PDA. Of note, *Ern1*/Ire1α inactivation is embryonic lethal, while *Ern2*/Ire1β-deficient mice are viable, indicating functional differences between the two paralogs.[60–62] Our data suggest that the development of Agr2- and Ire1β-specific inhibitors could be beneficial for the treatment of PDAs of the classical subtype and potentially other mucus-secreting tumours.

RNA-based subtypes are beginning to inform treatment strategies for patients. Clinical trials such as PASS-01 (NCT04469556) are ongoing to directly evaluate the efficacy of standard-of-care chemotherapy in PDA patients with classical-like versus basal-like-predominant metastatic PDA.[63] Here, we identified a classical-to-basal-like phenotype switch in PDA tumours that was triggered by inactivation of the SPDEF programme. Our data indicated that understanding cell state evolution during therapy is important to prevent relapse, and drug combinations that suppress distinct cell states may be required to overcome resistance and enhance overall responses. Future studies should be aimed at directing pancreatic cancer cell differentiation into cell states that can be eradicated therapeutically.

Acknowledgements We thank Taehoon Han and Erika Wee for assistance with statistical analyses and microscopy, respectively. This work was performed in collaboration with the Cold Spring Harbor Laboratory shared resources, which are supported by the National Institutes of Health (Cancer Center Support Grant 5P30CA045508: Bioinformatics, DNA Sequencing, Flow Cytometry, Animal, Animal and Tissue Imaging Shared Resources). This work was performed with assistance from the US National Institutes of Health Grant S10OD028632-01.

Contributors Conceptualisation: CT, GNY and DAT; Methodology: CT; Investigation: CT, GNY, EB, ADoshi and JP; Formal analysis and interpretation of data: CT, YH, ADeschênes, JH, OK, PB, ADobin and JP; Resources: RHH, OK and CRV; Writing–original draft: CT; Writing–review and editing: CT, GNY, ADeschênes, YH, OK, RHH, YP and DAT; Visualisation: CT; Funding acquisition: CT, YP and DAT; Supervision: YP and DAT; Guarantor of the project: DAT.

Funding The authors are supported by the Lustgarten Foundation, where DAT is a distinguished scholar and Director of the Lustgarten Foundation–designated Laboratory of Pancreatic Cancer Research. DAT is also supported by the Thompson Foundation, the Pershing Square Foundation, the Cold Spring Harbor Laboratory and Northwell Health Affiliation, the Northwell Health Tissue Donation Program, the Cold Spring Harbor Laboratory Association, and the National Institutes of Health (5P30CA45508, U01CA210240, R01CA229699, U01CA224013, 1R01CA188134, and 1R01CA190092). This work was also supported by a gift from the Simons Foundation (552716 to DAT). CT was a fellow of the American-Italian Cancer Foundation. YP is supported by the National Cancer Institute (R50CA211506).

Competing interests CRV has received consulting fees from Flare Therapeutics, Roivant Sciences, and C4 Therapeutics, has served on the scientific advisory board of KSQ Therapeutics, Syros Pharmaceuticals, and Treeline Biosciences, has received research funding from Boehringer-Ingelheim and Treeline Biosciences, and has received a stock option from Treeline Biosciences outside of the submitted work. DAT is a member of the Scientific Advisory Board and receives stock options from Leap Therapeutics, Surface Oncology, and Cygnal Therapeutics and Mestag Therapeutics outside the submitted work. DAT is scientific cofounder of Mestag Therapeutics. DAT has received research grant support from Fibrogen, Mestag and ONO Therapeutics. DAT receives grant funding from the Lustgarten Foundation, the NIH and the Thompson Foundation.

Patient and public involvement Patients and/or the public were not involved in the design, or conduct, or reporting, or dissemination plans of this research.

Patient consent for publication Not applicable.

Provenance and peer review Not commissioned; externally peer reviewed.

Data availability statement Data are available in a public, open access repository. The full list can be found in online supplemental materials and methods. Further information and requests for resources and reagents should be directed to the lead contact, Dr. David A. Tuveson dtuveson@cshl.edu.

ORCID iDs
Astrid Deschênes http://orcid.org/0000-0001-7846-6749
David A Tuveson http://orcid.org/0000-0002-8017-2712

REFERENCES

1 Siegel RL, Miller KD, Wagle NS, *et al*. Cancer statistics, 2023. *CA Cancer J Clin* 2023;73:17–48.
2 Distler M, Aust D, Weitz J, *et al*. Precursor lesions for sporadic pancreatic cancer: Panin, IPMN, and MCN. *Biomed Res Int* 2014;2014:474905.
3 Guerra C, Barbacid M. Genetically engineered mouse models of pancreatic adenocarcinoma. *Mol Oncol* 2013;7:232–47.
4 Waddell N, Pajic M, Patch A-M, *et al*. Whole genomes redefine the mutational landscape of Pancreatic cancer. *Nature* 2015;518:495–501.
5 Collisson EA, Sadanandam A, Olson P, *et al*. Subtypes of pancreatic ductal adenocarcinoma and their differing responses to therapy. *Nat Med* 2011;17:500–3.
6 Moffitt RA, Marayati R, Flate EL, *et al*. Virtual microdissection identifies distinct tumor- and stroma-specific subtypes of Pancreatic Ductal adenocarcinoma. *Nat Genet* 2015;47:1168–78.
7 Bailey P, Chang DK, Nones K, *et al*. Genomic analyses identify molecular subtypes of pancreatic cancer. *Nature* 2016;531:47–52.
8 Cancer Genome Atlas Research Network. Electronic address: andrew_aguirre@dfci.harvard.edu, Cancer Genome Atlas Research Network. Integrated genomic characterization of pancreatic ductal adenocarcinoma. *Cancer Cell* 2017;32:185–203.
9 N Kalimuthu S, Wilson GW, Grant RC, *et al*. Morphological classification of pancreatic ductal adenocarcinoma that predicts molecular subtypes and correlates with clinical outcome. *Gut* 2020;69:317–28.
10 Chan-Seng-Yue M, Kim JC, Wilson GW, *et al*. Transcription phenotypes of pancreatic cancer are driven by genomic events during tumor evolution. *Nat Genet* 2020;52:231–40.
11 Hayashi A, Fan J, Chen R, *et al*. A unifying paradigm for transcriptional heterogeneity and squamous features in pancreatic ductal adenocarcinoma. *Nat Cancer* 2020;1:59–74.
12 Miyabayashi K, Baker LA, Deschênes A, *et al*. Intraductal transplantation models of human pancreatic ductal adenocarcinoma reveal progressive transition of molecular subtypes. *Cancer Discov* 2020;10:1566–89.
13 Raghavan S, Winter PS, Navia AW, *et al*. Microenvironment drives cell state, plasticity, and drug response in pancreatic cancer. *Cell* 2021;184:6119–37.
14 Hanahan D. Hallmarks of cancer: new dimensions. *Cancer Discov* 2022;12:31–46.
15 Hingorani SR, Wang L, Multani AS, *et al*. Trp53R172H and KrasG12D cooperate to promote Chromosomal instability and widely metastatic pancreatic ductal adenocarcinoma in mice. *Cancer Cell* 2005;7:469–83.
16 Hingorani SR, Petricoin EF, Maitra A, *et al*. Preinvasive and invasive ductal pancreatic cancer and its early detection in the mouse. *Cancer Cell* 2003;4:437–50.
17 Lamouille S, Xu J, Derynck R. Molecular mechanisms of epithelial-mesenchymal transition. *Nat Rev Mol Cell Biol* 2014;15:178–96.
18 Rhim AD, Mirek ET, Aiello NM, *et al*. EMT and dissemination precede pancreatic tumor formation. *Cell* 2012;148:349–61.
19 Muzumdar MD, Dorans KJ, Chung KM, *et al*. Clonal dynamics following p53 loss of heterozygosity in Kras-driven cancers. *Nat Commun* 2016;7:12685.
20 Baslan T, Morris JP, Zhao Z, *et al*. Ordered and deterministic cancer genome evolution after p53 loss. *Nature* 2022;608:795–802.
21 Tonelli C, Deschênes A, Yao MA, *et al*. Loss of p53 tumor suppression function drives invasion and genomic instability in models of murine pancreatic cancer. *Cancer Biology* [Preprint] 2022.
22 Pitter KL, Grbovic-Huezo O, Joost S, *et al*. Systematic comparison of pancreatic ductal adenocarcinoma models identifies a conserved highly plastic basal cell state. *Cancer Res* 2022;82:3549–60.
23 Carstens JL, Yang S, Correa de Sampaio P, *et al*. Stabilized epithelial phenotype of cancer cells in primary tumors leads to increased colonization of liver metastasis in Pancreatic cancer. *Cell Rep* 2021;35:108990.

24 Gregorieff A, Stange DE, Kujala P, *et al*. The ETs-domain transcription factor Spdef promotes maturation of goblet and Paneth cells in the intestinal epithelium. *Gastroenterology* 2009;137:1333–45.
25 Chen G, Korfhagen TR, Xu Y, *et al*. SPDEF is required for mouse pulmonary goblet cell differentiation and regulates a network of genes associated with mucus production. *J Clin Invest* 2009;119:2914–24.
26 Chen G, Korfhagen TR, Karp CL, *et al*. FoxA3 induces goblet cell metaplasia and inhibits innate antiviral immunity. *Am J Respir Crit Care Med* 2014;189:301–13.
27 Schlesinger Y, Yosefov-Levi O, Kolodkin-Gal D, *et al*. Single-cell Transcriptomes of Pancreatic Preinvasive lesions and cancer reveal Acinar Metaplastic cells' heterogeneity. *Nat Commun* 2020;11:4516.
28 Burdziak C, Alonso-Curbelo D, Walle T, *et al*. Epigenetic plasticity cooperates with cell-cell interactions to direct pancreatic tumorigenesis. *Science* 2023;380:eadd5327.
29 Ma Z, Lytle NK, Chen B, *et al*. Single-cell transcriptomics reveals a conserved metaplasia program in pancreatic injury. *Gastroenterology* 2022;162:604–20.
30 McCauley HA, Liu C-Y, Attia AC, *et al*. TGFbeta signaling inhibits goblet cell differentiation via SPDEF in conjunctival epithelium. *Development* 2014;141:4628–39.
31 Moniaux N, Andrianifahanana M, Brand RE, *et al*. Multiple roles of mucins in pancreatic cancer, a lethal and challenging malignancy. *Br J Cancer* 2004;91:1633–8.
32 Wang S, Kaufman RJ. The impact of the unfolded protein response on human disease. *J Cell Biol* 2012;197:857–67.
33 Higa A, Mulot A, Delom F, *et al*. Role of pro-oncogenic protein disulfide isomerase (PDI) family member anterior gradient 2 (AGR2) in the control of Endoplasmic Reticulum homeostasis. *J Biol Chem* 2011;286:44855–68.
34 Tirasophon W, Welihinda AA, Kaufman RJ. A stress response pathway from the endoplasmic reticulum to the nucleus requires a novel Bifunctional protein kinase/Endoribonuclease (Ire1P) in mammalian cells. *Genes Dev* 1998;12:1812–24.
35 Wang XZ, Harding HP, Zhang Y, *et al*. Cloning of mammalian IRE1 reveals diversity in the ER stress responses. *EMBO J* 1998;17:5708–17.
36 Maurer C, Holmstrom SR, He J, *et al*. Experimental Microdissection enables functional harmonisation of pancreatic cancer subtypes. *Gut* 2019;68:1034–43.
37 Carpenter ES, Elhossiny AM, Kadiyala P, *et al*. Analysis of donor pancreata defines the transcriptomic signature and microenvironment of early neoplastic lesions. *Cancer Discov* 2023;13:1324–45.
38 Sans M, Makino Y, Min J, *et al*. Spatial Transcriptomics of Intraductal papillary mucinous neoplasms of the Pancreas identifies Nkx6-2 as a driver of gastric differentiation and indolent biological potential. *Cancer Discov* 2023;13:1844–61.
39 Bell ATF, Mitchell JT, Kiemen AL, *et al*. Panin and CAF transitions in pancreatic carcinogenesis revealed with spatial data integration. *Cancer Biology* 2022.07.16.500312. [Preprint] 2022.
40 Tiriac H, Belleau P, Engle DD, *et al*. Organoid profiling identifies common responders to chemotherapy in pancreatic cancer. *Cancer Discov* 2018;8:1112–29.
41 Somerville TDD, Xu Y, Miyabayashi K, *et al*. Tp63-mediated enhancer Reprogramming drives the squamous subtype of Pancreatic Ductal adenocarcinoma. *Cell Rep* 2018;25:1741–55.
42 Diaferia GR, Balestrieri C, Prosperini E, *et al*. Dissection of transcriptional and cis-regulatory control of differentiation in human Pancreatic cancer. *EMBO J* 2016;35:595–617.
43 Laise P, Turunen M, Garcia AC, *et al*. Developmental and MAPK-responsive transcription factors drive distinct malignant subtypes and genetic dependencies in pancreatic cancer. *Cancer Biology* [Preprint].
44 Milan M, Balestrieri C, Alfarano G, *et al*. Pancreatic cancer cells require the transcription factor MYRF to maintain ER homeostasis. *Dev Cell* 2020;55:398–412.
45 Yuan H, Kajiyama H, Ito S, *et al*. ALX1 induces snail expression to promote epithelial-to-mesenchymal transition and invasion of ovarian cancer cells. *Cancer Res* 2013;73:1581–90.
46 Muckenhuber A, Berger AK, Schlitter AM, *et al*. Pancreatic ductal adenocarcinoma subtyping using the biomarkers hepatocyte nuclear factor-1A and cytokeratin-81 correlates with outcome and treatment response. *Clin Cancer Res* 2018;24:351–9.
47 Buchwalter G, Hickey MM, Cromer A, *et al*. PDEF promotes Luminal differentiation and acts as a survival factor for ER-positive breast cancer cells. *Cancer Cell* 2013;23:753–67.
48 Turner DP, Moussa O, Sauane M, *et al*. Prostate-derived ETS factor is a mediator of metastatic potential through the inhibition of migration and invasion in breast cancer. *Cancer Res* 2007;67:1618–25.
49 Feldman RJ, Sementchenko VI, Gayed M, *et al*. PDEF expression in human breast cancer is correlated with invasive potential and altered gene expression. *Cancer Res* 2003;63:4626–31.
50 Wang F, Koul S, Shanmugam PST, *et al*. Prostate-derived Ets factor (PDEF) inhibits metastasis by inducing epithelial/luminal phenotype in prostate cancer cells. *Mol Cancer Res* 2018;16:1430–40.
51 Gu X, Zerbini LF, Otu HH, *et al*. Reduced PDEF expression increases invasion and expression of Mesenchymal genes in prostate cancer cells. *Cancer Res* 2007;67:4219–26.
52 Steffan JJ, Koul S, Meacham RB, *et al*. The transcription factor SPDEF suppresses prostate tumor metastasis. *J Biol Chem* 2012;287:29968–78.
53 Camolotto SA, Pattabiraman S, Mosbruger TL, *et al*. FoxA1 and FoxA2 drive gastric differentiation and suppress squamous identity in NKX2-1-negative lung cancer. *Elife* 2018;7:e38579.
54 Kloesch B, Ionasz V, Paliwal S, *et al*. A Gata6-centred gene regulatory network involving HNFs and ΔNp63 controls plasticity and immune escape in Pancreatic cancer. *Gut* 2022;71:766–77.
55 Dumartin L, Alrawashdeh W, Trabulo SM, *et al*. ER stress protein AGR2 precedes and is involved in the regulation of Pancreatic cancer initiation. *Oncogene* 2017;36:3094–103.
56 Tsuru A, Fujimoto N, Takahashi S, *et al*. Negative feedback by IRE1BETA optimizes mucin production in goblet cells. *Proc Natl Acad Sci U S A* 2013;110:2864–9.
57 Martino MB, Jones L, Brighton B, *et al*. The ER stress transducer IRE1Beta is required for airway epithelial Mucin production. *Mucosal Immunol* 2013;6:639–54.
58 Cloots E, Simpson MS, De Nolf C, *et al*. Evolution and function of the epithelial cell-specific ER stress sensor IRE1Beta. *Mucosal Immunol* 2021;14:1235–46.
59 Grey MJ, De Luca H, Ward DV, *et al*. The epithelial-specific ER stress sensor ERN2/IRE1B enables host-microbiota crosstalk to affect colon goblet cell development. *J Clin Invest* 2022;132:e153519.
60 Urano F, Bertolotti A, Ron D. Ire1 and Efferent signaling from the endoplasmic reticulum. *J Cell Sci* 2000;113 Pt 21:3697–702.
61 Iwawaki T, Akai R, Yamanaka S, *et al*. Function of Ire1 alpha in the placenta is essential for placental development and embryonic viability. *Proc Natl Acad Sci U S A* 2009;106:16657–62.
62 Bertolotti A, Wang X, Novoa I, *et al*. Increased sensitivity to dextran sodium sulfate colitis in IRE1Beta-deficient mice. *J Clin Invest* 2001;107:585–93.
63 O'Kane GM, Grünwald BT, Jang G-H, *et al*. Gata6 expression distinguishes classical and basal-like subtypes in advanced pancreatic cancer. *Clin Cancer Res* 2022;28:2715.